Journal of Thermal Analysis and Calorimetry, Vol. 78 (2004) 227–237

THERMAL DECOMPOSITION BEHAVIOUR OF LANTHANUM(III) TRIS-TARTRATO LANTHANATE(III) DECAHYDRATE

N. Deb[*]

Department of Chemistry, North Eastern Regional Institute of Science and Technology,
Nirjuli 791109, Itanagar, Arunachal Pradesh, India

(Received August 10, 2003; in revised form November 6, 2003)

Abstract

Lanthanum(III) tris-tartrato lanthanate(III) decahydrate, $La[La(C_4H_4O_6)_3]\cdot 10H_2O$ has been synthesized and characterized by elemental analysis, IR, electronic spectral and X-ray powder diffraction studies. Thermal studies (TG, DTG and DTA) in air showed a complex decomposition pattern with the generation of an anhydrous species at ~170°C. The end product was found to be mainly a mixture of La_2O_3 and carbides at ~970°C through the formation of several intermediates at different temperature. The residual product in DSC study in nitrogen at 670°C is assumed to be a similar mixture generated at 500°C in TG in air. Kinetic parameters, such as, E^*, ΔH, ΔS, etc. obtained from DSC are discussed. IR and X-ray powder diffraction studies identified some of the decomposition products. The tentative mechanism for the thermal decomposition in air of the compound is proposed.

Keywords: IR, lanthanum tartrato complex, thermal decomposition, X-ray powder diffraction

Introduction

Many workers [1–4] have studied tartrates of transition and non-transition metals of different types. Structure determinations have been made on numerous crystalline tartrate complexes and coordination patterns have been reviewed [5, 6]. The tartrate coordination in crystal structure of $(NMe_4)_2[MoO_2(C_4H_4O_6)_2]EtOH\cdot 1.5H_2O$ has been investigated [7]. Gel grown pure and mixed rare earth tartrates [8] of yttrium and samarium are found to be decomposed to their stable oxides. The carboxylate precursor, magnesium tris(maleato)ferrate(III)dodecahydrate has found [9] to decompose to different intermediates i.e. α-Fe_2O_3 and MgO through the formation of magnesium maleate. Further, magnesium ferrite, $MgFe_2O_4$ is generated through a solid–solid reaction of MgO and α-Fe_2O_3 at 600°C, a temperature much lower than the ceramic method. The complexes of 2,3-dimethoxy benzoates of heavy lanthanides and yttrium of the type $Ln(C_9H_9O_4)_3\cdot nH_2O$ are studied [10], where the complexes of Tb(III),

---

[*] Author for correspondence:E-mail: nidhubandeb@yahoo.com

1388–6150/2004/ $ 20.00

Akadémiai Kiadó, Budapest
Kluwer Academic Publishers, Dordrecht

Dy(III), Ho(III), Er(III), Tm(III) and Y(III) are found to produce the oxides of the respective metals at 1273 K in air through the formation of anhydrous salts, whereas Yb(III) and La(III) are directly decomposed to the oxides. The carboxylate coordination compounds of iron, nickel and zinc with malates are reported [11] to produce α-Fe_2O_3, NiO and ZnO as end products in air through the formation of anhydrous malates, malonates, oxoacetates (iron and nickel compounds) and hydroxocarbonate (zinc compound) as intermediates. We have synthesized and studied extensively the thermal behaviour of carboxylato complexes with oxalate as ligand of the type $M[M(C_2O_4)_n]\cdot xH_2O$ [12–16] (where *M*=same metal), $M_3[La(C_2O_4)_3]\cdot xH_2O$ [17, 18] (where *M*=Li, Na and K), $M_1[M_2(C_2O_4)_2]\cdot xH_2O$ [19] (where M_1=Co or Cd, M_2=Ni) and $M[La(C_2O_4)_3]\cdot H_2O$ [20] (where *M*=Cr or Co), where various interesting decomposition phenomena are observed leading to different products. Although, the oxalato complexes of various types are reviewed [21] and studied, the carboxylato complexes with tartrate as ligand are less reported. Although there had been a report [22] on tartrato complexes of the type $M[M(tart)_n]\cdot xH_2O$ (where *M*=Co(II)), and keeping in mind the formation of different intermediates and end products and their possible catalytic applicability the paper reports the synthesis, characterization and thermal decomposition of lanthanum(III) tris-tartrato lanthanate(III) decahydrate, $La(III)[La(III)(C_4H_4O_6)_3]\cdot 10H_2O$ in air and nitrogen media. The tentative mechanism for the decomposition in air has also been proposed.

Experimental

All the chemicals used were of AR grade purity. We followed the same preparative method adopted for oxalato complexes [14–18]. Lanthanum nitrate was converted to chloride by digesting repeatedly with concentrated hydrochloric acid. The chloride free hydroxide was then produced by washing several times with distilled water. It was dissolved in glacial acetic acid and heated on a steam bath. A white compound was precipitated by dropwise addition of a saturated solution of tartaric acid. The compound was separated from solution and washed several times with distilled water and air dried at ambient temperature, then stored in a desiccator. Water and metal contents were determined thermogravimetrically and gravimetrically [23] by known methods.

Microanalytical data were recorded with a Carlo Erba 1108 elemental analyser. IR spectra of the compound and the intermediates were recorded from 200 to 4000 cm^{-1} in nujol mulls with a Perkin Elmer 883 spectrophotometer. Diffuse reflectance spectrum was measured with Shimadzu UV-240 spectrophotometer using $BaSO_4$ as the reference material. TG, DTG and DTA profiles were recorded in static air at a heating rate of 10°C min^{-1} using Shimadzu DT 30B thermal analyzer. DSC was carried out in dynamic nitrogen up to 670°C using Perkin Elmer PC series DSC-7 at a heating rate of 10 and 15°C min^{-1}. The kinetic parameters of the phase transformation processes were determined after integration of the peaks. Powder X-ray diffraction (XRD) of the compound and decomposition products was obtained using a Geigerflex microprocessor controlled automated Rigaku (Japan) X-ray diffractometer system D/Max IIIC with SASG accessory.

Results and discussion

The complex, La(III)[La(III)($C_4H_4O_6$)$_3$]·10H_2O is obtained as white powder and is insoluble in water or in common organic solvents. However, it decomposes in strong acid or alkali. The water analysis revealed that the compound contains ten molecules of water. Analytical and microanalytical results were consistent with the proposed molecular formula of the complex. As *vs.* the calculated composition (in mass%) of La, 30.79; C, 15.98; H, 3.58; H_2O, 19.97, the analysis showed La, 30.43; C, 16.30; H, 3.62; H_2O, 19.35. Selected bands in the IR spectrum of the complex are included in Table 1. The chelating character of the carboxylate (tartrato) group as well as the presence of coordinated and crystal water was concluded on the basis of earlier studies [1, 3, 15, 22, 24]. The electronic spectrum of the solid sample showed the bands around 27.390 and 46.500 cm^{-1} which are due to L→M charge transfer and intraligand $\pi\rightarrow\pi^*$ transition, respectively. The XRD pattern (Table 2) of the compound indicates its crystalline nature.

Table 1 Selected bands in the IR spectrum of La(III)[La(III)($C_4H_4O_6$)$_3$]·10H_2O

IR bands^a/cm^{-1}	Assignments
2400–4000 (b)	ν_{sy}(O–H)+ν_{asy}(O–H) of water or hydrogen bonding
(Centered at 3420)	ν(O–H) of free hydroxyl of tartrato group
1300–1720 (mb) (centered at 1600)	ν_{asy}(C=O) and/or δ_{sy}(H–O–H)
1380 (S)	ν_{sy}(C–O)+ν(C–O) and/or δ(O–C=O)
1080 (m), 1110 (m)	Alcoholic C–O stretching vibration
710 (s)	Coordinated water
640 (s)	ν(La–O) and/or ν(C–C) or water of crystallisation
560 (s)	ν(La–O) and/or ν(C–C)
480 (vs)	Ring deformation and/or ν(O–C=O)
400 (vs)	ν(O–C=O)
305 (m)	Out-of-plane bending

^{a}s – small; vs – very small; m – medium; S – strong; b – broad

The thermal profiles (TG, DTG and DTA) of La[La($C_4H_4O_6$)$_3$]·10H_2O at 10°C min^{-1} in air are shown in Fig. 1. The TG curve shows a continuous mass loss from room temperature to 1000°C with several breaks indicating the formation of several intermediates. An inclined slope upto 170°C with a mass loss of 20% (calculated, 19.97%) indicates the elimination of all ten molecules of water. DTG change between room temperature and 180°C and an endothermic peak in DTA in the range 53–162°C (ΔT_{min}=78°C) with a small shoulder peak at 146°C are due to the dehydration step. The shoulder at 146°C may be due to removal of coordinated water molecules. The anhydrous form loses mass of 2% upto 260°C, which apparently indi-

Table 2 X-ray powder diffraction data of La(III)[La(III)$(C_4H_4O_6)_3$]·$10H_2O$, and its pyrolysed products in air

La[La$(C_4H_4O_6)_3$]·$10H_2O$		Product at 355°C		Product at 500°C		Product at 805°C		Product at 970°C	
d/Å	*I*/%	*d*/Å	*I*/%	*d*/Å	*I*/%	*d*/Å	*I*/%	*d*/Å	*I*/%
8.109	100.00	5.904	83.32	8.322	73.04	5.794	76.75	5.762	100.00
3.782	86.27	5.724	89.63	5.762	70.70	3.259	100.00	3.241	89.96
2.648	75.43	3.360	100.00	4.302	78.32	3.220	40.10	3.030	26.18
2.419	76.62	2.190	87.02	2.991	100.00	2.304	51.65	2.344	40.00
2.198	78.77	1.651	58.80	2.970	68.21	1.886	61.00	2.278	60.23
2.018	75.62	1.520	57.11	2.941	70.21	1.642	56.21	2.291	59.46
1.799	48.62	1.369	56.89	2.072	65.10	1.605	26.42	2.240	42.12
1.381	37.40	1.330	71.23	2.049	77.54	1.491	36.46	1.882	69.50
1.319	37.11	1.186	45.30	1.478	49.14	1.457	26.66	1.840	36.10
1.233	36.28	1.177	60.23	1.457	53.20	1.428	31.06	1.658	16.22
1.144	37.62	1.093	43.57	1.356	50.23	1.362	28.19	1.490	30.28
1.083	34.04	0.996	39.29	1.330	39.44	1.260	35.10	1.457	18.53
1.047	34.96	0.917	38.34	1.277	40.10	1.236	28.44	1.428	20.19
0.951	31.87	0.913	40.26	1.156	38.30	1.177	19.84	1.328	11.97
0.931	31.50	0.907	52.14	1.177	43.62	1.107	17.26	1.357	38.26
0.885	33.34	0.893	44.19	1.052	37.41	1.090	26.10	1.309	22.12

Table 2 Continued

$La[La(C_4H_4O_6)_3]\cdot 10H_2O$		Product at 355°C		Product at 500°C		Product at 805°C		Product at 970°C	
d/Å	*I*/%	*d*/Å	*I*/%	*d*/Å	*I*/%	*d*/Å	*I*/%	*d*/Å	*I*/%
0.833	42.70	0.875	39.89	0.984	37.90	1.075	32.10	1.260	30.20
0.819	40.18	0.828	50.26	0.934	40.12	1.035	18.79	1.240	18.92
0.806	38.35	0.820	47.13	0.929	37.63	0.991	16.88	1.187	33.28
0.787	39.60	0.805	54.15	0.898	38.78	0.946	17.26	1.173	12.74
		0.791	48.77	0.874	35.23	0.936	38.26	1.102	12.36
				0.848	42.12	0.891	26.22	1.065	18.23
				0.840	41.35	0.844	17.69	1.040	13.51
				0.825	45.49	0.828	18.20	0.948	8.88
				0.814	40.76	0.822	22.14	0.916	11.97
				0.798	44.62	0.808	19.84	0.858	10.81
						0.805	22.00	0.844	19.23
						0.803	20.74	0.839	10.81
						0.785	23.26	0.833	13.13
								0.817	13.51
								0.793	15.06

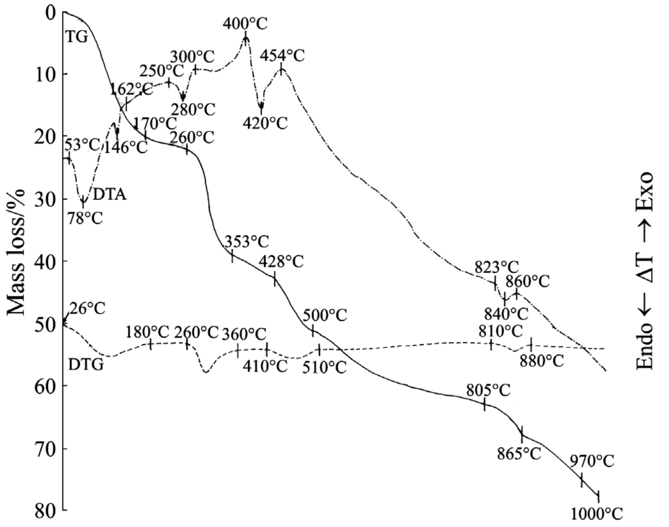

Fig. 1 TG, DTG and DTA curves of La(III) [La(III)$(C_4H_4O_6)_3$]·$10H_2O$ in air at 10°C min^{-1}

cates the formation of La[La$(C_4H_4O_6)_{2.85}$ and led to the cumulative mass loss of 22% (calculated value 22.43%). The intermediate is not stable in TG and decomposed to subsequent products at 353°C through partial breaking of $C_4H_4O_6^{2-}$ anion of the anhydrous moiety. The partial rupture of the bidentate group with evolution of CO(*g*) and CO_2(*g*) is also attributed in other studies [15, 17]. An endotherm in the range 250–300°C (ΔT_{min}=280°C) in DTA may be responsible for the initiation of rupture of tartrato group and possible rearrangement. The IR bands of the residue isolated from the compound preheated to 250°C in furnace are found mostly in similar with the precursor, which give credence to the retention of coordinated tartrato groups. Further, another distinct slope in TG from 260 to 353°C with 39% cumulative mass loss apparently suggests that the intermediate is either an oxalate of lanthanum, La[La$(C_2O_4)_3$] (calcd. mass loss, 39.94%); or, a mixture of $1/2La_2O_3$, and $1/2La_2(C_4H_4O_6)_x$ (where x=3) (calcd. mass loss, 41.93%). The difference between the observed and calculated mass loss to get the residue may be due to the presence of free unoxidised C [28, 29] and it compounds in trace. Corresponding to the above changes, a sharp change in the range 260–360°C in DTG and an exotherm of ΔT_{max} of 400°C followed by an overlapping endotherm of ΔT_{min} of 420°C in DTA are displayed.

As the powder XRD data (Table 2) of the pyrolysed product at ~355°C in furnace does not coincide with the data obtained [15] for lanthanum oxalate, the possibility of its formation can be ignored. In the case of cobalt tartrate complex, however, the existence of mixture of cobalt oxalate and oxide was proposed [22] at 360°C through the formation of cobalt meso oxalate at ~220°C. The powder XRD data of the product isolated at ~355°C confirmed [25] the presence of La_2O_3 along with traces of LaCO, La_2C_3 and C (carbon). The carbon formed due to disproportionation [18] of the evolved

CO(g) during the rupture of $C_4H_4O_6^{2-}$ groups partially could react even at the low temperature, producing [15] carbide (La_2C_3) and oxycarbide (LaCO). The remaining mismatched d-values in the XRD data of the mixture species at 355°C might be the possible rearranged products of $1/2La_2(C_4H_4O_6)_x$ (where x=3 or <3). The IR band at 1300–1720 cm^{-1} that contains the strong feature at 1580 cm^{-1} and associates with other features at 1385 (s), 1130 (s), 1082 (m), 940 (s), 860 (m), 780 (ms), 720 (s), 440 (ms), 400 (s), 376 (vs), 355 (vs) and 340 (vvs) cm^{-1} further substantiates the retention of bonds for characteristic vibration for tartrate groups. Terms written within brackets symbolise the strengths of IR peaks (for details refer Table 1). Some of the bands are for the species of lanthanum [17, 30] formed at 355°C in furnace. Like earlier study [17] observed in the case of $Na_3[La(III)(C_2O_4)_3]\cdot 8H_2O$, the rapid conversion of an exothermic change at 400°C to an endotherm at 420°C and subsequently to a broad exotherm at ~454°C are exhibited in the DTA of this study. These are attributed [26] to the partial decomposition of tartrate groups with the evolution of CO(g), and exothermic conversion of a part of CO(g) to CO_2(g) at 400°C. The separation of $1/2La_2O_3$ and $1/2La_2(C_4H_4O_6)_3$ from one mole of tartrate and their rearrangement took place at 420°C; and their subsequent decomposition manifested exothermically in accordance with 454°C. The observed mass loss in TG in the range of 353–428°C may be due to decomposition of $La_2(C_4H_4O_6)_x$(s) with the release of gaseous products and the solid–solid interaction of the intermediates formed at ~353°C. A part of solid carbon generated at 353°C may be oxidised to CO(g) and CO_2(g), which may also lead to mass loss. Further, a change in DTG (410–510°C) which corresponds to a steep slope in TG in the range 428–500°C attaining 51% cumulative mass loss suggests that the product may be a mixture of $1/2La_2O_3$ with $1/2La_2(C_2O_4)_3$, the oxalate (calcd. mass loss, 51.91%) or $LaC_4H_2O_5$, the meso oxalate [22] (calcd. mass loss 52.13%) from one mole of the tartrate. The exotherm in DTA displayed at 454°C is due to the decomposition of $1/2La_2(C_4H_4O_6)_3$, which was formed at 353°C. The XRD data (Table 2) of the pyrolysed greyish black product at 500°C confirmed the existence of La_2O_3 along with a trace of La_2C_3 and LaCO. But the XRD data does not match with reported [15] data of lanthanum oxalate; instead a few d-values coincided with the d-values of lanthanum oxycarbonate, $La_2O(CO_3)_2$. This suggests that the oxalate as soon as it formed as intermediate immediately decomposed to oxycarbonate, which is reported to be produced [15] at ~494°C from the precursor $La[La(C_2O_4)_3]\cdot 9H_2O$. Unlike earlier study [4, 22, 24], the possibility of formation of lanthanum meso oxalate, $LaC_4H_2O_5$ as intermediate could not be observed. In this context, the dioxycarbonate, $La_2O_2CO_3$ may also be formed through the trapping [28] of CO_2(g) with a part of porosive La_2O_3. Some mismatched d-values gives the credence to the formation of dioxycarbonate, $La_2O_2CO_3$, which also might be produced directly from the decomposition of lanthanum oxalate (transient in this study), or from the slow conversion of a part of the oxycarbonate within 500°C. However, our earlier study [15] reported it to be formed at 526°C. The medium to small IR bands at 1640 (s), 1600 (m), 1360–1550 (centered at 1386), 845 (m), 765 (s), 720 (s), 400 (vs), 340 (vvs) and 310 (vvs) cm^{-1} of the isolated species at 500°C could be attributed due to the presence of CO_3^{2-} group [18] and other products. The product at 500°C gave effervescence with hydrochloric acid, which indicates the existence of carbonate. Further, the continuous mass loss in TG even after 500°C suggests the slow conversion of oxycarbonate and dioxycarbonate to the oxide, La_2O_3, where the earlier generated La_2O_3 may act as catalyst. We isolated the pyrolysed product at 805°C and its XRD patterns (Table 2) confirmed the presence of La_2O_3, La_2C_3, LaCO and La. The absence of *d*-values of oxy and dioxycarbonate indicates the complete transformation to oxide within 805°C. The multiple IR absorption bands observed at 1640 (s), 1386 (m), 1360 (m), 1085 (vs), 765 (vs), 645 (mS), 580 (mS), 400 (vs), 375 (vs), 340 (vvs), 310 (vvs) cm^{-1}, having similarity to the bands of the product obtained at 500°C further substantiates the presence of the oxide, carbide and oxycarbide of lanthanum. An endotherm in the DTA in the range of 823–860°C (ΔT_{min} at 840°C) and the mass loss till a TG break at 865°C with cumulative loss of 67.5% may be due to the solid–solid reaction of the products contemplated at 805°C, which in turn, may be converted to some other products with continuous mass loss upto the limit of the scanning at 1000°C. Eventually, the 78% mass loss at 1000°C gives the hint of the tendency of formation of metallic lanthanum. Prior to the formation of residue at 1000°C, we isolated the pyrolysed species at ~970°C in furnace, and the XRD data (Table 2) still confirmed the presence of La_2O_3, La_2C_3, LaCO and a trace of La.

The DSC profile of the compound in nitrogen at 10°C min^{-1} is shown in Fig. 2. The profile displayed three endothermic peaks. We enlarged the endotherms for kinetic analysis by changing the heat flow axis. The first endotherm between 52.12 to 166.68°C is accounted for the dehydration step, followed by another endothermic peak in the range 251.62–318.48°C may be corroborating to the partial breaking of the tartrato groups. The study suggests that the anhydrous compound be formed both in nitrogen and air approximately at similar temperature. The kinetic parameters evaluated after integration of the peaks is included in Table 3. The high activation energy (E^*) for the second step indicative [15] of the slow fragmentation of anhydrous

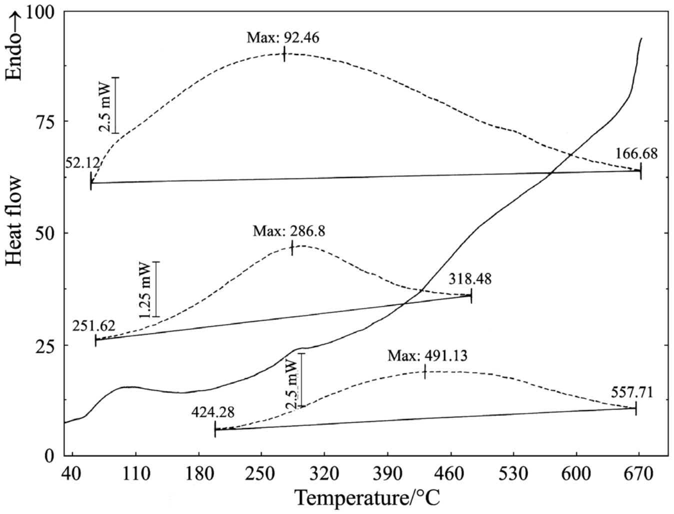

Fig. 2 DSC curves of La(III) $[La(III)(C_4H_4O_6)_3]\cdot 10H_2O$ in nitrogen at 10°C min^{-1}

Table 3 DSC data of La(III)[La(III)$(C_4H_4O_6)_3$]$\cdot 10H_2O$ in nitrogen

Heating rate/ °C min^{-1}	Step	Temp. range/°C	Peak temp./°C	lnk_0/s^{-1}	E^*/kJ mol^{-1}	ΔH/ kJ mol^{-1}	ΔS/ J K^{-1} mol^{-1}	Order of reaction	Reaction
10	1	52.12–166.68 (endo)	92.46	5.04±0.10	32.58±0.70	398.56	1090.57	0.87±0.01	dehydration
	2	251.62–318.48 (endo)	286.80	61.36±1.32	305.47±6.59	49.26	88.00	1.37±0.02	decomposition
	3	424.28–557.71	491.13	31.49±0.68	234.21±5.06	163.57	221.91	1.17±0.02	decomposition

species. Further, another flat endotherm between 424.28 to 557.71°C indicates further rapid decomposition of the intermediates with low E^* as compared to second step. The 50.71% mass loss at the end of the scanning upto 670°C may be due to the formation of similar product formed at 500°C in TG in air. From the Table 3 the values of change of enthalpy (ΔH) and entropy (ΔS) seem to be dependent on the area of the endotherms of the respective changes. The low value of ΔH and ΔS of the 2nd endothermic peaks supports the partial breaking of the $C_4H_4O_6^{2-}$ moiety, whereas comparatively the large value of ΔH and ΔS of last peaks indicates the rapid decomposition of the intermediates to oxide and oxycarbonate/dioxycarbonate through the complete rupture of all the metal–ligand bonds.

The foregoing results suggest the following tentative decomposition scheme in air.

$$\mathrm{La[La(C_4H_4O_6)_3]\cdot 10H_2O} \xrightarrow{\text{room temp.} - 170^\circ\mathrm{C}} \mathrm{La[La(C_4H_4O_6)_3]}(s)+10\mathrm{H_2O}(g) \xrightarrow{\sim 260^\circ\mathrm{C}}$$

$$\mathrm{La[La(C_4H_4O_6)_x]}(s)\ (\text{where } 2<x<3)+1\mathrm{CO}(g) \xrightarrow{\sim 353^\circ\mathrm{C}}$$

$$1/2\mathrm{La_2O_3}(s)+1/2\mathrm{La_2(C_4H_4O_6)_x}(s)(\text{where } x=3 \text{ or } <3)+\mathrm{LaCO}(s)(\text{trace})+$$

$$\mathrm{La_2C_3}(s)(\text{trace})+\mathrm{C}(\text{trace})+m\mathrm{CO}(g)+n\mathrm{CO_2}(g) \xrightarrow{428-500^\circ\mathrm{C}}$$

$$1/2\mathrm{La_2O_3}(s)+\mathrm{La_2O(CO_3)_2}(s)/\mathrm{La_2O_2CO_3}(s)+$$

$$\mathrm{LaCO}(s)+\mathrm{La_2C_3}(s)+p\mathrm{CO}(g)+q\mathrm{CO_2}(g)+r\mathrm{C_2H_4}(g) \xrightarrow{\sim 805^\circ\mathrm{C}}$$

$$\mathrm{La_2O_3}(s)+\mathrm{La_2C_3}(s)+\mathrm{LaCO}(s)+\mathrm{La}(s)\ (\text{trace})+x\mathrm{CO}(g)+y\mathrm{CO_2}(g) \xrightarrow{\sim 970^\circ\mathrm{C}}$$

$$\mathrm{La_2O_3}(s)(\text{trace})+\mathrm{La_2C_3}(s)(\text{trace})+\ \mathrm{LaCO}(s)(\text{trace})+\mathrm{La(s)}(\text{trace})$$

* * *

The author is thankful to Dr N. Sen Sarma, Dibrugarh University, Assam for recording the DTA-TG profile, Dr S. D. Baruah of Regional Research Laboratory, Jorhat, Assam for DSC profile and Head, RSIC, CDRI, Lucknow for elemental analysis.

References

1 S. Kirschner and R. Kiesling, J. Am. Chem. Soc., 20 (1960) 4174.
2 N. Dennis Chasteen and R. Linn, Inorg. Chem., 9 (1970) 169.
3 P. E. Rush, J. D. Oliver and G. D. Simpson, J. Inorg. Nucl. Chem., 37 (1975) 1393.
4 R. I. Valiullina and K. P. Prilylov, Russ. J. Inorg. Chem., 36 (1991) 3.
5 N. H. Pilkington and R. Robson, Aust. J. Chem., 23 (1970) 2225.
6 S. Groh, Israel J. Chem., 15 (1976/77) 277.
7 W. T. Robinson and C. J. Wilkins, Trans. Met. Chem., 11 (1986) 86.
8 A. Jain, S. Bhat, S. Pandita, M. L. Kaul and P. N. Kotru, Proc. 11th Nat. Symp. Therm. Anal., Jammu, India, March 2–5, (1998) 103.
9 B. S. Randhawa and K. J. Sweety, J. Therm. Anal. Cal., 65 (2001) 829.
10 W. Ferenc and A. Walkow-Dziewulska, J. Therm. Anal. Cal., 71 (2003) 375.
11 L. Patron, O. Carp, I. Mindru, G. Marinescu and E. Segal, J. Therm. Anal. Cal., 72 (2003) 281.
12 N. Deb, P. K. Gogoi and N. N. Dass, Bull. Chem. Soc. Jpn., 16 (1988) 4485.

13 N. Deb, P. K. Gogoi and N. N. Dass, J. Thermal Anal., 35 (1989) 27.
14 N. Deb, S. D. Baruah and N. N. Dass, J. Thermal Anal., 45 (1995) 457.
15 N. Deb, S. D. Baruah, N. Sen Sarma and N. N. Dass, Thermochim. Acta, 320 (1998) 53.
16 N. Deb, S. D. Baruah, N. Sen Sarma and N. N. Dass, Thermochim. Acta, 329 (1999) 129.
17 N. Deb, S. D. Baruah and N. N. Dass, Thermochim. Acta, 326 (1999) 43.
18 N. Deb, Thermochim. Acta, 338 (1999) 27.
19 N. Deb, S. D. Baruah and N. N. Dass, J. Therm. Anal. Cal., 59 (2000) 791.
20 N. Deb, J. Therm. Anal. Cal., 67 (2002) 699.
21 K. V. Krishnamurty and G. M. Harris, Chem. Rev., 61 (1961) 213.
22 S. Sarmah and N. N. Dass, J. Thermal Anal., 54 (1998) 913.
23 T. K. Sanyal and N. N. Dass, J. Inorg. Nucl. Chem., 42 (1980) 811.
24 P. N. Ketru, N. K. Gupta, K. K. Raina and I. B. Sharma, J. Mater. Sci., 21 (1986) 83.
25 Joint Committee on Powder Diffraction Standards, Inorganic Index to the Powder Diffraction File, 1971, 1601, Parklane, Pennsylvania.
26 P. S. Bassi, B. S. Randhawa and S. Kaur, Indian J. Chem., A, 31 (1992) 596.
27 S. Prasad, A. Vijayalakshmi and N. S. Gajbhiye, J. Thermal Anal., 52 (1998) 595.
28 G. M. Bancroft, K. G. Dharmawardena and A. G. Maddok, Inorg. Chem., 9 (1970) 223.
29 B. S. Randhawa and Randhir Singh, Thermochim. Acta., 243 (1994) 101.
30 F. F. Bently, L. D. Smithson and A. L. Rozek, Infrared Spectra and Characteristic Frequencies, 300–700 cm^{-1}, Wiley, New York 1968.